

Generation of Microbubbles for Biomedical Applications through an Automated Microfluidic Setup



By

MUNIBAH QURESHI

NUST201362087MSMME62413F

Supervised by: Dr. Murtaza Najabat Ali

**School of Mechanical and Manufacturing Engineering
National University of Sciences and Technology
H-12 Islamabad, Pakistan
December, 2015**

Generation of Microbubbles for Biomedical Applications through an Automated Microfluidic Setup

A thesis submitted in partial fulfillment of the requirement for the
degree of Masters of Science

In
Biomedical Sciences and Engineering

By
MUNIBAH QURESHI
NUST201362087MSMME62413F

Supervised by: **Dr. Murtaza Najabat Ali**

**School of Mechanical and Manufacturing Engineering
National University of Sciences and Technology
H-12 Islamabad, Pakistan**

December, 2015

DECLARATION

It is hereby declared that this research study has been done for partial fulfillment of requirements for the degree of Masters of Sciences in Biomedical Sciences. This work has not been taken from any publication. I hereby also declare that no portion of the work referred to in this thesis has been submitted in support of an application for another degree or qualification in this university or other institute of learning.

Munibah Qureshi

Every breath of my life and drop of blood in my body is dedicated to my family to whom I owe everything.

ACKNOWLEDGEMNT

“In the name of Allah the most Merciful and Beneficent”

First and foremost, praises and thanks to Allah, the Almighty, who is my Lord and who is my all who never let efforts go wasted. His blessings and guidance throughout made me complete this project successfully.

I don't have words to thank to my family to whom I owe everything, the ones who can never ever be thanked enough, for the overwhelming love and care they bestow upon me. Without their proper guidance it would have been impossible for me to complete my study. Thanks to my sisters for their encouragement affection, support, care, prayers and giving me real happiness whenever I am depressed, to my grandmother and aunts for their consistent prayers and care.

I would like to express my profound and sincere gratitude to my research supervisor, Dr. Murtaza Najabat Ali, for giving me the opportunity to work under his supervision. His timely contribution, encouragement, kindness and valuable advices helped me shape my work into its final form. My sincere appreciation goes to my Co supervisor Dr. Shahrukh Abbas for valuable guidance and suggestions. Indeed, her feedback and constructive comments were really helpful.

I am also deeply indebted to my committee members especially to Dr. Umar Ansari for kindness in examining the research work and providing suggestions for improvement and for generously supporting the thesis with his expertise throughout. Thanks to Dr Adeeb shahzad for his encouragement, advices and moral support and Dr. Nabeel Anwar for his helpful criticism, comments and administrative support.

Special thanks right from the depth of my heart to Abdul Rehman and Amad Ahmad from School of Electrical Engineering and Computer Sciences (SEECS) for their sincere and efficient contribution, Muhammad Irfan Azam for his friendly assistance with various problems all the time especially in paper work.

I would like the whole hearted thank my friend Amber Zahoor who helped me passionately and sincerely, Tanzeela Noreen Alvi who has listened to my moaning and complaining, Bakhtawer

Ghafoor for helping me in writing and to all my lab fellows for providing me friendly and peaceful environment in whole tenure of my research work.

The special thanks goes to DD MRC, each and every technician at MRC, lab staff of Prosthetics Lab, Biochemistry lab SMME, SCME and ASAB lab staff for their Kind assistance.

Last but not the least, I would like to thank each and every person for supporting me throughout this research phase in any way.

PUBLICATIONS

Javeria Sami, Murtaza Ali, **Munibah Qureshi**, Irfan Azam, Umer Ansari, Mariam Mir, Biodegradable polymeric composite material for biomedical applications-A Review; IRBM (2015) 9submitted)

Munibah Qureshi, Murtaza Najabat Ali, Shahrukh Abbas, Umer Ansari, Irfan Azam, Amber Zahoor,, Recent Advancements in microfluidic devices (2015)
(to be submitted)

TABLE OF CONTENTS

LIST OF FIGURES	viii
LIST OF TABLES	x
ABBREVIATION	xi
Abstract	1
1. INTRODUCTION	2
1.1 Components of Microbubbles	3
1.1.1. Gas Phase	3
1.1.2 Shell Material	4
2. LITERATURE REVIEW	5
2.1 MB generation techniques	5
2.1.1 Sonication	5
2.1.2 High shear emulsification	5
2.1.3 Membrane emulsification	5
2.2 Microfluidic devices	6
2.2.1 Flow focusing device	7
2.2.2 T-junction MFDs	10
2.2.3 Co-Flow Microfluidic Devices	13
3. MATERIALS AND METHODS	15
3.1 Design and Fabrication of Syringe Pump	15
3.1.1 Designing	15
3.1.2 Fabrication	16
3.1.3 Calibration of Syringe Pump	19
3.2 Design and Fabrication of Microfluidic device	20
3.2.1 Designing	20
3.2.2.1 Acrylic slabs	21
3.2.2.2 Polyurethane casting	22
3.2.2.3 Teflon tubes	23
3.3 Microbubble generation	24
3.4 Characterization	26
4. RESULTS AND DISCUSSION	27
4.1 Design and Fabrication of syringe pump	27

4.1.1 Calibration	28
4.2 Design and Fabrication of Microfluidic Device	29
4.3 Microbubble generation and Characterization	32
4.3.1 Optical microscopic images	32
4.3.2 Polydispersity index	33
5. CONCLUSION	36
REFERENCES	37

LIST OF FIGURES

Figures	Titles	Page No.
Figure 1a	Components of microbubbles (b) Microbubbles	3
Figure 2a	Microfluidic setup Figure 2b Microfluidic device geometry and bubbling process	6
Figure 3	(a) Combined T-junction and flow focusing microfluidic device (FFT) (b) Image showing microbubbles encapsulated in water droplets in FFT (c) DFF Microfluidic device (d) Illustration of water droplet Encapsulated microbubbles in DFT	8
Figure 4	Flow focusing devices of different angles	10
Figure 5	Capillary embedded T-junction MF device with the appropriate dimensions To produce MBs	11
Figure 6	T junction MF chip, showing delivery of three phases	12
Figure 7	Pro E model of syringe pump	15
Figure 8	Laser engraving	16
Figure 9	(a) Assembled parts (b) Plunger mover along with part to fix the plunger and nut affixed for screw (c) Ball bearing attached in acrylic part (d) Cap on syringe holding holes for screw (M4) (e) Syringe holder and screws for fixation of cap	17
Figure 10	M6 threaded rod coupled to shaft of stepper motor through aluminum coupling	18

Figure 11	Assembled syringe pump	18
Figure 12	Complete syringe pump assembly along with circuit material encased in box, Keypad for input and LED	19
Figure 13	MF flow focusing device design	20
Figure 14	MF T-junction device design	21
Figure 15	Channels fabricated on acrylic slabs	22
Figure 16	(a) Master mold of acrylic sheet (b) silicon mold (c) PU 744D (d) Two PU 744D sealed together making patterns of channels	23
Figure 17	Crosslinking of chitosan with glutaraldehyde	24
Figure 18	(a) MB generation through automated microfluidic setup (b) Closed view of bubbles inside flowing in outlet	25
Figure 19	Final assembled syringe pump	27
Figure 20	Graph showing flow rates at various number of steps	28
Figure 21	(a) MF T junction device (b) MF T junction protected by casting PU 744 D	29
Figure 22	A complete MF setup (a) Power supply (b) Syringe pump for gas phase (c) Syringe pump for liquid phase (d) MF device (e) Bubbles generated through this setup	31
Figure 23	Microscopic images of 1%, 2% chitosan collected in three different glutaraldehyde concentrations	32
Figure 24	(a) 1% chitosan Bubbles shrinking with time (b) 2% chitosan bubbles shrinking with time	35

LIST OF TABLES

Table 1	Laser parameters and depth achieved	22
Table 2	Average size of chitosan bubbles	33
Table 3	Stability of chitosan bubbles	34

ABBREVIATION

MBs	Microbubbles
mm	Millimeter
µm	Micrometer
dm	Diameter
µl	Microliter
ml	Milliliter
MF	Microfluidics
%	Percent
MEMS	Micro Electro Mechanical System
TCAS	Total Chemical Analysis System
LOC	Lab on Chip
PDMS	Polydimethylsiloxane
PMMA	Poly methyl methacrylate)
FFT	Flow focusing T junction
DFE	Double Flow Focusing
FFMD	Flow focusing microfluidic device
kV	Kilo volts
PAN	Polyacrylonitrile
SDS	Sodium dodecyl sulphate
PEG	Polyethylene glycol

UV	Ultraviolet
PLA	Poly Lactic Acid
PU	Polyurethane
rpm	Revolution per minute
PCB	Printed circuit boards

Abstract

Microbubbles are bubbles with diameters less than 1mm. They have gained significant attention in various medical and non-medical applications including ultrasonic imaging, diagnosis, drug delivery, food processing, water treatment and surface cleaning. Conventional techniques such as ultra-sonication, mechanical agitation and membrane emulsification etc., produce microbubbles with less monodispersity because of reduced control over size and uniformity. Microfluidic approaches offer major improvements in terms of control over shape, size and uniformity. The aim of this project was to develop a cost-effective microfluidic setup for the generation of micro-bubbles. The setup consists of syringe pumps for controlled flow rate and a microfluidic device fabricated using Teflon tubes. Air-filled chitosan microbubbles were generated successfully using this MF setup, within the narrow size range of 200 μ m to 260 μ m. Polydispersity index value of chitosan MBs calculated was 6% that was quite good than polydispersity indices achieved through conventional techniques. Future work can be carried out to further scale down the size of bubble so that they can be used for biomedical applications.

1. INTRODUCTION

Microfluidic devices have received substantial consideration during recent years because of the exact control of fluids in small volume and multiphase flows [1] [2]. The emergence of microfluidics at the end of 1970's lead to the progress of micro electromechanical systems (MEMS) using microelectronic knowledge [3]. The idea of miniaturized total chemical analysis system (TCAS) which is also called as micro total chemical analysis system (micro-TCAS) was presented by Manz et al in 1990. Later on in 1992 Harrison et al named this technique as laboratories on a chip (LOC). Soon after the fabrication of LOC, the first practical application in analytical chemistry was to differentiate sample constituents [4] [5] [6]

In the modern era, microfluidic devices due to their high proficiency, controllability and safety are being employed in emulsification, biochemistry, gas purification, material synthesis, processes of chemical reaction and for generation of micro sized droplets and bubbles. [7] [8].

Common microbubble generating techniques are sonication [9], high shear emulsification [10], excimer laser ablation and inkjet printing. Major problem with these techniques is monodispersity [11] which depends upon the physical and chemical properties of fluids, control of flow rates of fluids streams and the geometry of microfluidic devices. [12] [13]. Therefore to eliminate larger bubbles further filtration steps are required.

Microbubbles are very small bubbles of size ranging from 1 to few microns and remain separate from each other means do not aggregate and remain suspended in a suitable medium for prolonged period [14] Keeping in mind the rheology of the red blood cells in micro vessels and capillaries the size of the microbubbles must be equal to the red blood cells; that is less than 10 μ m [15] Different Microfluidic approaches have been developed for microbubble generation to meet emerging medical and pharmaceutical demands. By decreasing the internal diameter of the micro channels and width of the outlet in microfluidic devices, microbubbles of size less than 10 μ m can be obtained [16][17].

A substantial growth has been made in the development of microbubbles because of their medical and industrial applications. Their use as theranostics extend the horizon towards biomedical applications as they react to ultrasound waves which makes them useful in molecular imaging,

targeted gene and drug delivery and contrast ultrasound imaging for various purposes. Application other than these comprise water treatment, food processing, surface cleaning, enhanced oil recovery, material synthesis They improve the fermentation of soil, hydroponic plant growth, and aquaculture productivity[18][14]

1.1 Components of Microbubbles

Basically Microbubbles comprise of 3phases

1.2.1 Inner Gas Phase

1.2.2. Outer Shell Encapsulating Gas Phase

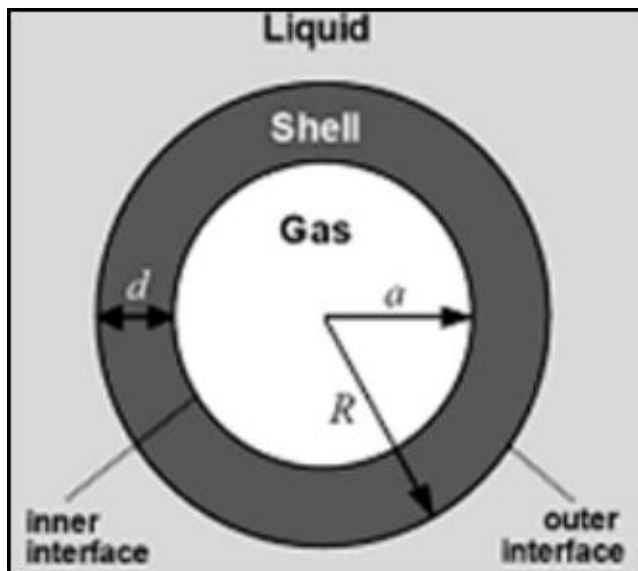


Figure1a: Components of microbubbles [14]



Figure 1b: Microbubbles

1.1.1. Gas Phase

The gas phase or core can be a single gas or a combination of gases. Use of mixture gases stabilize the bubbles. Upon exposure to ultrasonic waves, the gas core expands during the rarefaction phase and during compression it contracts. Ultrasound parameters, are known to effect several phenomena to occur that enable ultrasound backscatter or targeted drug delivery from the microbubble shell. Phenomena range from acoustic radiation force to very energetic processes like

inertial cavitation. Coaction of all these events enables imaging, targeting, precise release and vascular permeability improvement. [14]

1.1.2 Shell Material

The shell material enclose the gas phase. It can be of proteins, lipids and polymers [15]. Shell has a key role in the mechanical properties of MB along with diffusion of gas out of the bubble. The shell also provide site for drug loading, ligand to attain targeting. It accounts for the elasticity. If it is more elastic more acoustic energy it can endure before rupturing so increases the stability. [14]

2. LITERATURE REVIEW

2.1 MB generation techniques

2.1.1 Sonication

Mostly used technique for MB generation is sonication that involves ultrasound to agitate liquid or gas particles in the suspension of an appropriate coating material [9] [19]. Frequency, pulse and power of ultrasound effect the size range of bubbles. Size distribution obtained through sonication is very broad [20]. It is generally necessary to remove large bubbles through filtration to be injected intravenously.[21]

2.1.2 High shear emulsification

This method is mainly for generating microbubbles of polymer coating. Method involves emulsification of polymer dissolved in an aqueous suspension through high shear stirring,[10] and by using one more liquid that act as stabilizer and is immiscible with polymer and volatile solvent that will evaporate soon , causing the formation of core inside from droplets to form polymer coated microspheres. To remove excess solvent additional washing step is done and then microspheres are freeze dried to generate gas filled MBs [22]. MBs size distribution depends droplets in the early emulsion and on any disintegration or amalgamation during successive processing. Again additional filtration step is required to obtain narrow size range for biomedical applications [23]

2.1.3 Membrane emulsification

MBs are generated in this technique through a porous membrane [24]. First liquid droplets are prepared and then treated to form microbubbles as described above or formed directly using gas as dispersed phase [25]. This technique offers good control over MB size than obtained through sonication or shear emulsification,[26] without effecting the yield. Though it depends upon membrane characteristics [27] [16], are largely dependent on the properties of the membrane such

as wettability, pore sizes and surface treatment, but the narrow size distribution is again hard to attain[28][18].

2.2 Microfluidic devices

MF have been used for generation of MBs with precisely controlled dimensions. The size of bubbles can be controlled by controlling flow rates and viscosities of the liquids, the pressure of the gas stream, and the orifice size [17]. Flow rate is controlled through “syringe pumps” that introduce the liquid and gas at constant flow rate. Orifice is the crucial feature of device at which gas phase intrudes upon a flow of liquid and is focused to outlet like a jet. Consequently, at some distance beginning the orifice, the interface of gas liquid becomes unbalanced and bubbles formation occurs like a “pinch-off” mechanism (Figure 2b) [29]. MF devices enable generation of bubbles in a single step and can also generate bubble with multilayered coatings. For example, recently MBs coated with a mixture of gold nanoparticles and surfactant has been generated by fabricating T-junction device [30].

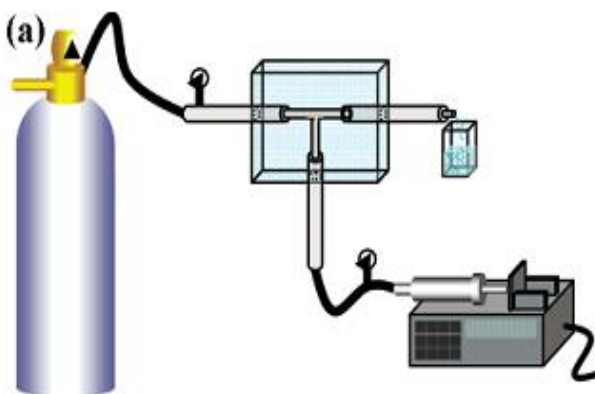


Figure 2a: Microfluidic setup

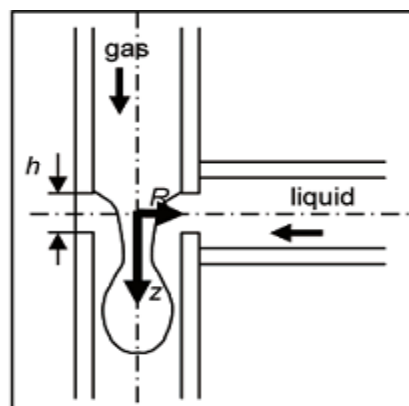


Figure 2b: Microfluidic device geometry and
Bubbling process

Basic geometries of microfluidic devices for microbubble generation are Flow-focusing devices, T-junction devices [31] and co-flow (coaxial capillaries) devices[32]. Mostly lithography techniques are utilized for fabrication of device on polydimethylsiloxane (PDMS), PMMA and Polyurethane etc. Currently, photolithography, laser cutting and engraving and chemical wet etching are usually used for fabrication of 2D microfluidic devices [20].

Modifications in microfluidic devices have been made and effects on generation has been studied Here is recent progress made in microfluidic devices.

2.2.1 Flow focusing device

In flow focusing device two immiscible fluids are poured down into three inlet channels such that the liquids from both sides surround the gas from central channel. These strike at the junction of the channel upstream to the outlet orifice. This assembly is extensively used for microbubble generation[33] and is still being modified for specific applications. xt. Gan ~ an-Calvo & Gordillo reported the production of bubbles using this geometry for the first time. Using cylindrical gas tubes and controlling the flow ratios of gas and liquid, resulted in the production of about 10 micrometer monodisperse bubbles. Arrangement of the inlet tube and the outer orifice was not so clear. Anna et al first established a prevalent type of planar flow focusing for generation of emulsions [34]; the same geometry was used for microbubble generation by Garstecki et al [35].Hettiarachchia et al carried out a detailed study and generated monodisperse microbubbles with polydispersity index (σ) of <2% and diameter <5 μm , through MF flow-focusing device having 7 micro meter orifice. Reducing the gas inlet and orifice distance resulted in a decrease in pressure required to generate the same bubble volumes at a persistent flow rate of liquid. [16].Yaoyao et al fabricated a flow focusing chip on a block of super white glass. Monodispersed microbubbles of sizes <5 μm and well defined radial tolerances were achieved. [33].

Wan and his coworkers further modified the device and MF devices of two unlikely geometries, T-junction and a flow focusing were combined as shown in (fig. 1). FFT (flow focusing followed by T-junction), had advantage an over DFF (double flow focusing) in that it can regulate the amount of bubbles per droplet of water while DFF forms comparatively thin water layer around every single microbubble. [36]

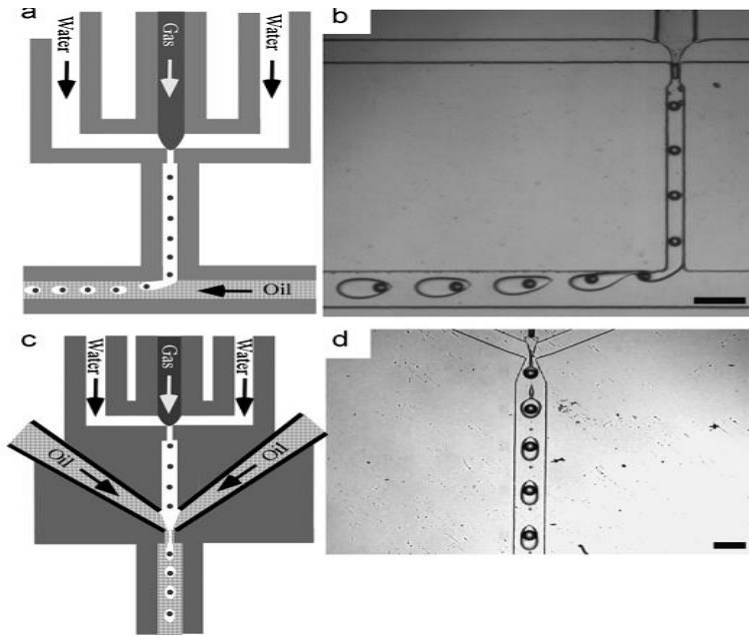


Figure 3: (a) combined T-junction and flow-focusing microfluidic device (FFT). (b) Image showing microbubbles encapsulated in water droplets in FFT. (c) (DFF) the double flow-focusing microfluidics device (d) illustration of water droplet encapsulated microbubbles in DFT. [36]

Taotao et al further studied the effect of several operating parameters like microchannel size, the gas, liquid flow rates and the liquid viscosities on the size of the bubble. Increasing width of microchannel increased the size of the bubble. This was detected for various liquid flow rates. Further, it was found that a broader microchannel resulted in extended formation time and larger bubble size with the same flow rate of liquid. [37]

Castro-Hernández et al described a procedure for the controlled generation of bubbles of $5\mu\text{m}$ size, below 5% polydispersity index and high production rates by fabricating a planar flow focusing device. It has very lengthy exit channels much larger than its width, which resulted in decrease in bubble in relation to the channel width, prevents obstruction of outlet channel and immensely reduce a pressure needed for injection of gas and liquids into microfluidic device. [38]

In another study, the FFMD is coupled to liquid full pressurized chamber, to skip tubing needed to inject liquid to microfluidic device. The technique made the FFMD fabrication and parallelization considerably simple. The smallest bubble size obtained was $7.1\pm 0.5\ \mu\text{m}$ and maximum generation rate was 333,000 MBs per second from a single nozzle which was increase further to 1.5 folds by using two nozzles. Along with improved production, flooded design also

permits miniaturization. [39] It was found that the device had to be connected to the external side of the pressurized chamber to avoid crumpling of the micro channels, which may possibly be improved by using a stiff alternates such as metal or glass instead of PDMS.[40]

Sally A. et al fabricated microfluidic flow focusing device that combine gas and liquid streams via very small nozzle of few microns and then injecting both phases to a pressure drop downstream for successful monodispersed generation of microbubbles that were clinically more applicable compared to traditional monodispersed microbubble populations. Microbubbles obtained were 2 micrometer in size. It was presented that, with increasing liquid flow rate, diameter of microbubbles decreased monotonically. As by equation

$$\frac{d}{D} \propto \left(\frac{Q_g}{Q_l} \right)^n \quad (1)$$

D is the diameter of nozzle and exponent “n” is affected by physical geometry of the device. For example, for axisymmetric geometries n differs between n =0.17 [41] and for flow focusing microfluidic devices with extended nozzles, n = 0.37[38]. It shows that diameter of bubble is largely dependent on geometry of device. S.Wang et al characterized PDMS based, two-dimensional planar, expanding rectangular nozzle for production of microbubbles. It was found that the production could not be sustained beyond one minute because FFMD was unstable in parameters used. Although the precise mechanism for the instability has not been explicated but it was assumed that unsystematic variations in the input parameters and fabricating material affected the FFMD.[42]

Salari et al focused on effect of angles between microchannels in flow focusing device and showed that, bubbles generation is governed by the shear tension, the liquid velocity in way to orifice increases which made the bubbles to produce away from the orifice position when angles are small. Increasing the angles between the channels decrease the shear tension outcome and increase the flow inertia effect as the relative velocity between liquid and air falls, for a fixed volume of gas the volume of liquid passing through the orifice is minimum and the bubbles are produced near to the orifice. Significant governing parameter at angle of 90 degrees is the flow inertia effect. Increasing an angle from this point would increase shear tension. The smallest and monodispersed bubbles were observed at 120 degrees. Figure 3 indicates that increase in an angle from 30 to 120

degree results in reduction in size of bubble. This phenomenon could be described by understanding relationship between shear and surface tension. [43]



Figure 4: Flow focusing devices of different angles [43].

Another flow-focusing microfluidic device was presented, having channels of specific height and width with nozzle diameter of $8\mu\text{m}$, which produced monodisperse microbubbles $8\mu\text{m}$ within the flow chamber. Blockage in this device was observed because of contamination during fabrication process but once the device started to generate bubbles contamination was not observed. Contamination issue can be resolved by incorporation of filters in channels [44]. These filters have also been used and caused stable production of microbubbles [45] [46].

2.2.2 T-junction MFDs

Fabrication and operating cost of T-junction devices is low, as they do not need specific clean environmental conditions and can easily be made using an acrylic block. The T-junction devices are less prone to deformation [47] so can be operated even at high pressure [30]. T-junction geometry is commonly deployed in chemical analysis [48] [49] screening conditions for protein crystallization [50], formation of solid non-spherical particles, microbubbles [51] and production of double emulsions [52]. It is the most widely used microchannel in microfluidic devices to produce immiscible fluid segments and microbubbles [53] [54]. Using crossflowing shear rupturing procedure in a T-junction microfluidic device, monodispersed MBs of $100\mu\text{m}$ to $500\mu\text{m}$ size and with polydispersity less than 2% were produced. [55]

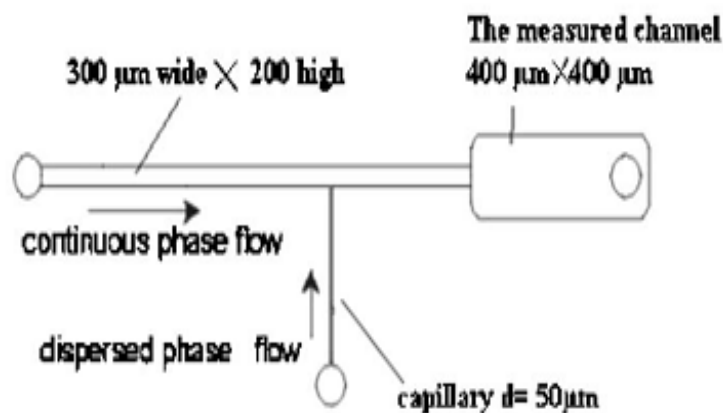


Figure 5. Capillary embedded T-junction microfluidic device with appropriate dimensions to produce MBs.[55]

A series of perpendicular flow routes with different angles varying from 30° to 150° to control the gas liquid dispersed flow in T-junction MF devices were developed. Flow pattern is shown to be dependent on the flow rate of both continuous phase and dispersed phase [2]. According to another study size of the MBs depends on the size of the external orifice. It was found that MBs of diameter less than $4.5\mu\text{m}$ can be generated by using a T-junction microchannel geometry made of polydimethylsiloxane (PDMS) combined with a thin capillary (as gas jet) having internal diameter of $2\mu\text{m}$. [28][30].

Eleanor and his coworkers presented that a single T-junction device can be used to generate number of different bubbles sizes only by varying the separation of capillaries to change the size of the orifice.[56].

Gas/liquid/liquid three phase monodispersed droplets and bubbles using double T-junction MF device were generated. First gas (air) / water (SDS 2 wt. %) plugs were formed; this two phase system was then used as a cross shearing fluid for oil (Hexane) at second T-junction. They also found that the breakup of oil droplet at second T-junction is mainly governed by cutting effect of the gas/liquid interface.[2][57]

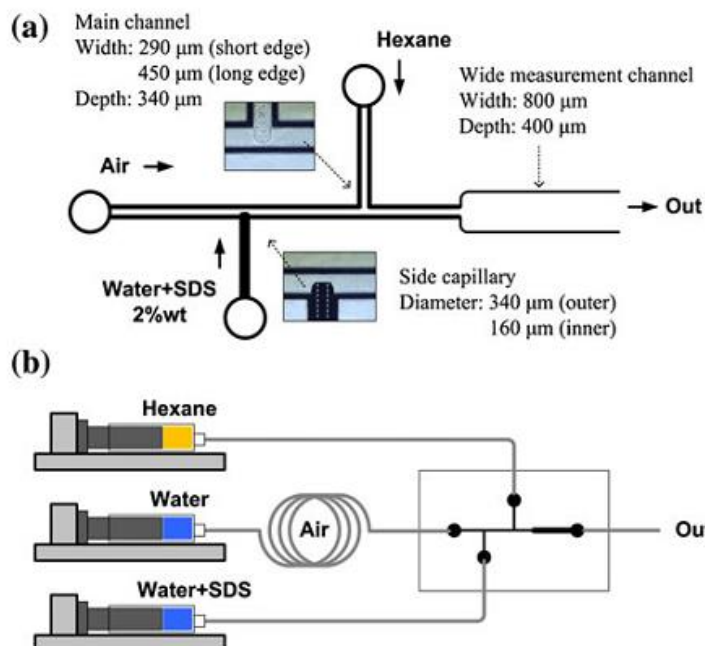


Figure 6. T-Junction micro fluid chip; showing delivery of three phases.[2]

K.Wang et al investigated that without changing the flow rates the dispersed sizes can be greatly reduced by low consumption of continuous phase and by extending length of capillary in the capillary embedded T junction MF device.[57]

In order to produce monodisperse MBs using triple T junction MF devices with several channel sizes, three coalescence behaviors were noticed i.e. absolute coalescence, non coalescence and probabilistic coalescence, mainly influenced by the liquid viscosities and two phase superficial velocity. Coalescence can generally be prevented by increasing liquid viscosity.[58]

M. Parhizkar et al., 2012 using T-junction microfluidic device produced MBs with polydispersity less than 1%. They further concluded that bubble size reduced with the increase of flow rate of liquid and viscosity while on the other hand it increases by increasing the gas pressure. They also investigated that bubble size depends on squeezing regime, dripping regime and geometry of the junction.[47]. In another work MBs with monodispersity $< 2\%$ in the capillary embedded T junction MF devices were investigated in order to determine the effect of different surfactants on their generation, size and stability. Nonionic surfactants, due to their high adsorption on to hydrophobic channel surface, produce more stable (150 days) and smaller MBs. Size of the MBs mainly depends on the wettability of the solution. [47]

It was found that when electrical potential difference about 12kV on outer channel of basic T-junction device was applied the size of MBs produced greatly decreased by ~25% of the capillary diameter while polydispersity index remains ~1% [59]. Another study demonstrated that double T junction MF devices can also be used to produce double emulsions i.e. water-in-oil-in-water and/or oil-in-water-in-oil (O1/W/O2) and hollow microspheres. The size of MBs can be controlled by slight adjustment in the liquid and gas flow rates. [60]

2.2.3 Co-Flow Microfluidic Devices

Break up in MF systems normally occurs in co flow device when both phases flow along the gradients of pressure and in confinement by walls of the devices.

Takasi Nisisako et al produced monodispersed bicolored “Janus particles” using Y-shaped channel in a planar glass chip to generate two-phase organic stream, integrated with co-flow geometry consisting of aqueous stream to produce biphasic droplets with coefficient of variation less than 2% [61]. Xiong et al experimentally and numerically investigated bubble formation process using co-flowing micro channels, made up of glass and silicon in a clean environment. They concluded that bubble break up and bubble length other than velocity distribution change around the barrier, highly dependent on the flow rate ratio of gas and liquid and also on the channel width and shape of bubble entirely depends upon the surface tension. Further they observed that this bubble break-up process in co-flowing microfluidic devices is similar to that of T-junction devices.[62]

J. H. Xu et al using co-flowing shear method in a co-axial microfluidic devices produced monodispersed chitosan microspheres having diameter ranging from 100 μ m to 700 μ m with polydispersity less than 4% and in situ solidification.[32]

W. van Hoeve and his team predicted that in spite of process parameters i.e. gas and liquid flow rates; the microbubble size highly depends on the radius of inner gas jet using co flowing MF device.[38]

Kai Wang et al prepared microbubbles diameter ranging from 391 μ m to 713 μ m with polydispersity less than 2.9% by using dispersed phase as propane, butane and air and continuous phase as SDS-PEG solutions; in co flowing MF device. They noticed two types of bubble

generation phenomenon called “single-bubble generation” flow and “double bubble generation” flow.[63]

Another effort using one-step double co-flowing capillary microfluidic devices generated monodispersed gas in water in oil (G/W/O) double emulsion. By means of this double emulsion as a soft templet and by UV-polymerization, they also generated hollow hydrogel microspheres with controllable structures.[64]

3. MATERIALS AND METHODS

Objectives of the study were

- Design and fabrication of Syringe pump
- Design and fabrication of microfluidic device
- Microbubble generation
- Characterization

3.1 Design and Fabrication of Syringe Pump

3.1.1 Designing

Model of syringe pump was first designed using Pro Engineer Wildfire 5.0.

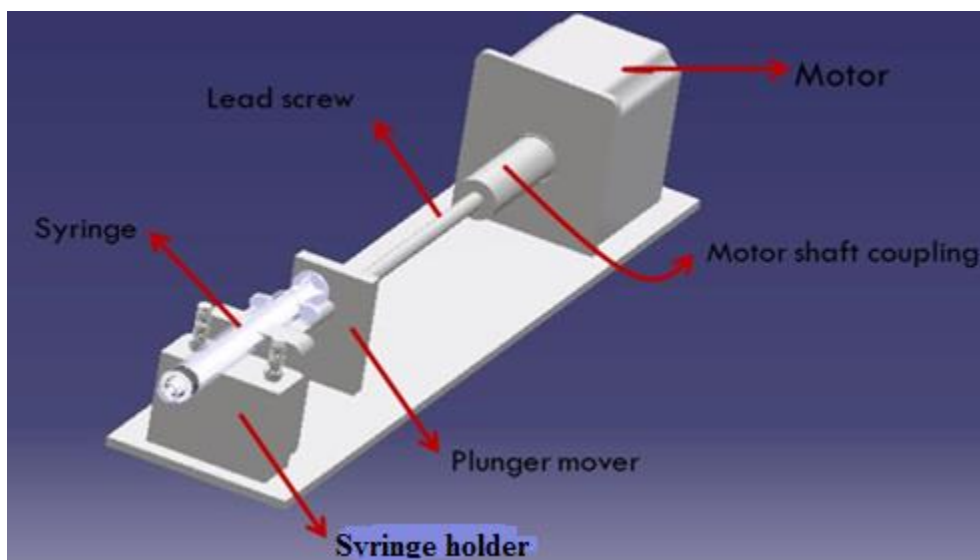


Figure 7: Pro E Model of syringe pump

The principle of a syringe pump is to use a fine-pitch leadscrew to move the plunger of a syringe, this was accomplished by using a stepper motor to actuate the plunger through stepper motor and a microcontroller to keep constant flow of fluids while holding the syringe body stationary.

Other parts were base on which all parts were fabricated, motor shaft coupling to couple leadscrew with motor shaft, part to fix the plunger, syringe holder to keep the syringe stationary through its cap.

3.1.2 Fabrication

Acrylic material was selected because it can easily be handled and cut into many shapes. The acrylic sheets of 4mm thickness were subjected to laser cutting and engraving, a computerized numerical (CNC) guided laser system (Shenzhen Lead CNC CNC-LS240A.). The designs used for Laser cutting were 2D design that was obtained by converting 3D Pro Engineer part file into AutoCAD ‘.dxf’ file that were directly imported into the system. So each part of assembly was first designed individually on Pro Engineering and then fabricated.

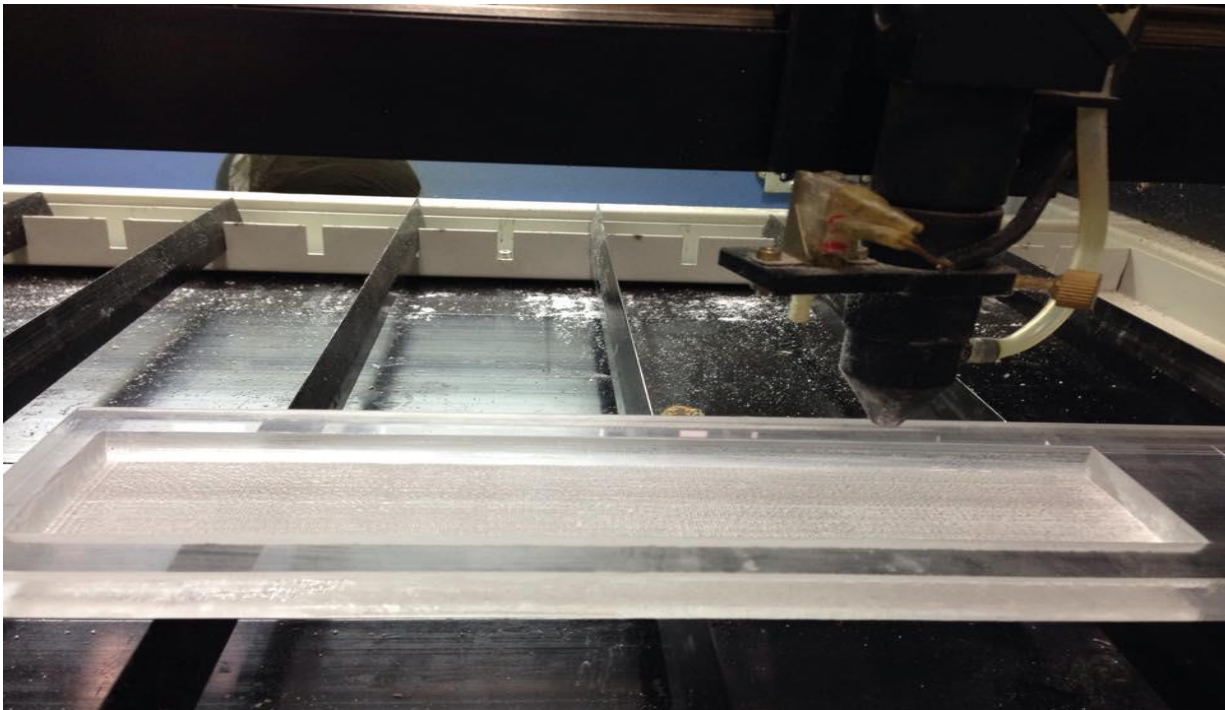


Figure 8:Laser engraving

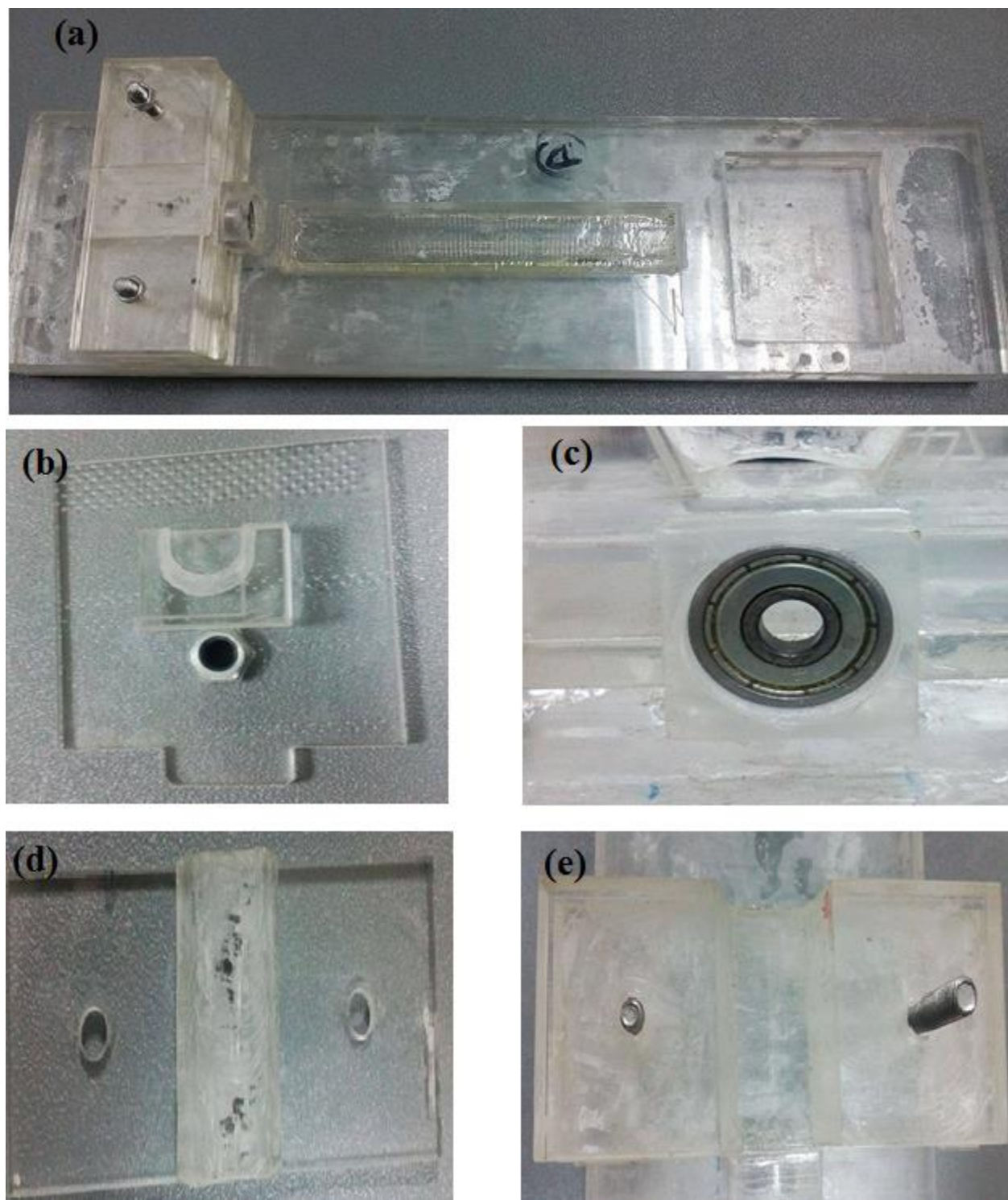


Figure 9: (a) Assembled parts (b) Plunger mover along with part to fix the plunger and nut affixed for screw (c) ball bearing attached in acrylic part (d) cap on syringe holding having holes for screw (M4) (e) syringe holder and screws for fixation of cap

Each part was exactly aligned and assembled around M6 threaded rod as the core structure of the assembly. Holes in syringe holder for M4 screws were made at Manufacturing Resource Centre, NUST (MRC) using BDQ5125 drill press and aluminum motor shaft coupling was also made at MRC using high speed lathe and milling machine. First the motor shaft coupling was made by PLA on 3D printer but that idea did not work well because of some flexibility of the polymer. M6 threaded rod was coupled to motor through this aluminum coupling.



Figure 10: M6 threaded rod coupled to shaft of stepper motor through aluminum coupling



Figure 11: Assembled syringe pump

Stepper motor used had wires working under maximum voltage supply of 12V and 1.93A Circuit was designed according to required flow rates using ARDUINO and a Stepper motor Driver Module. Number of steps were set with a time delay in mili seconds according to required speed. Required flow rates was given as an input to controller via keyboard. That could be seen on LED attached. Number of steps set for one revolution were 200 and lead screw had a pitch of

1mm, so one step was a plunger movement of $1/200=0.005\text{mm}$. Whole circuit was then encased in a box made of acrylic to avoid contact with circuit wiring. Keypad and LED was attached outside the box for giving input and display. The designed syringe pump is shown in figure 10.

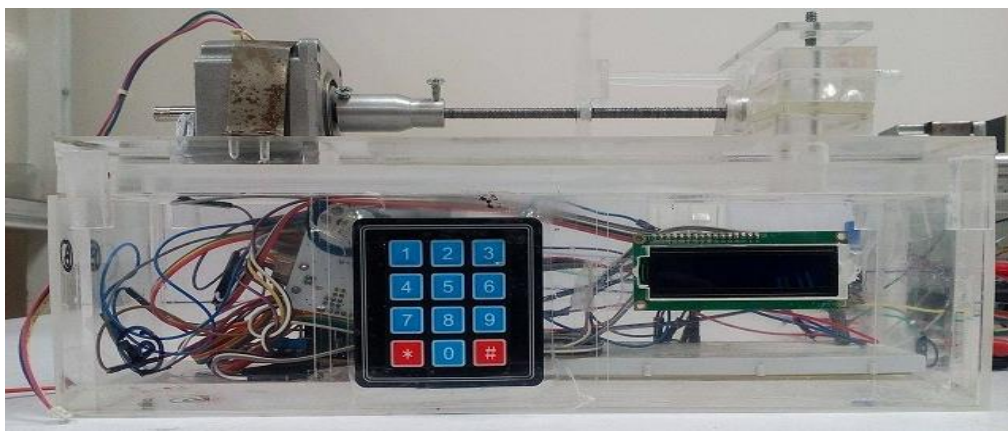


Figure 12: Complete syringe Pump assembly along with circuit material encased in box, Keypad for input and LED

3.1.3 Calibration of Syringe Pump

Calibration of syringe pump was done in order to attain a fix flow rate for liquid and gas. A 3 ml syringe was filled with distilled water without air entrapment. Starting from number of steps for one revolution that is 200, several number of steps were given at 60 seconds and volume of water ejected on different number of steps was noted by movement of plunger or distance covered by plunger from one point to other on graduated syringe. All steps were done in triplicates. Graphs were than plotted at several steps, for calculation of required flow rates.

3.2 Design and Fabrication of Microfluidic device

3.2.1 Designing

Microfluidic devices of two geometries were designed on Software Pro Engineer Wildfire 5.0. Geometries designed were flow focusing and T junction. Flow focusing geometry has three inlets one for gas and two for liquid or shell material and one outlet as shown in Figure. Over all dimension of device was 70mm × 90mm (length × width). The width of gas channel was kept less than liquid channels as gas has high diffusion rate of gas and also for formation of small bubbles it was desired.

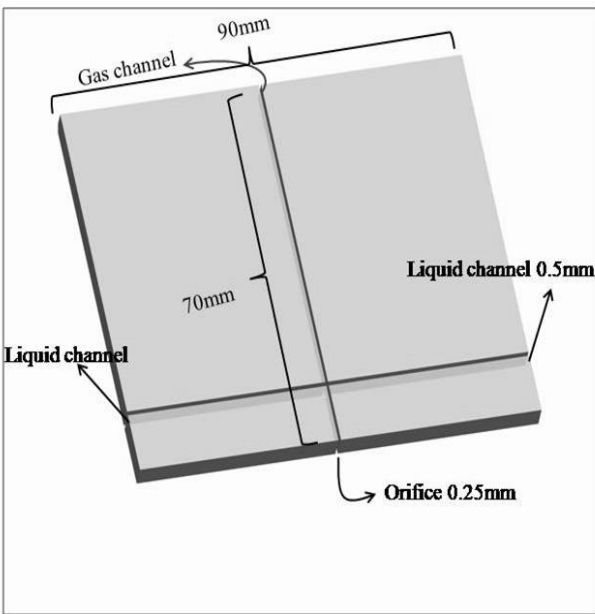


Figure 13: MF Flow focusing device design

T junction device geometry has two inlets. Inlet that is in line with outlet is for gas and the other that is perpendicular is for liquid or shell material as shown in figure. Again the width of gas Channel was kept less than liquid channel. Over all dimension of device was 70mm × 90mm (length × width)

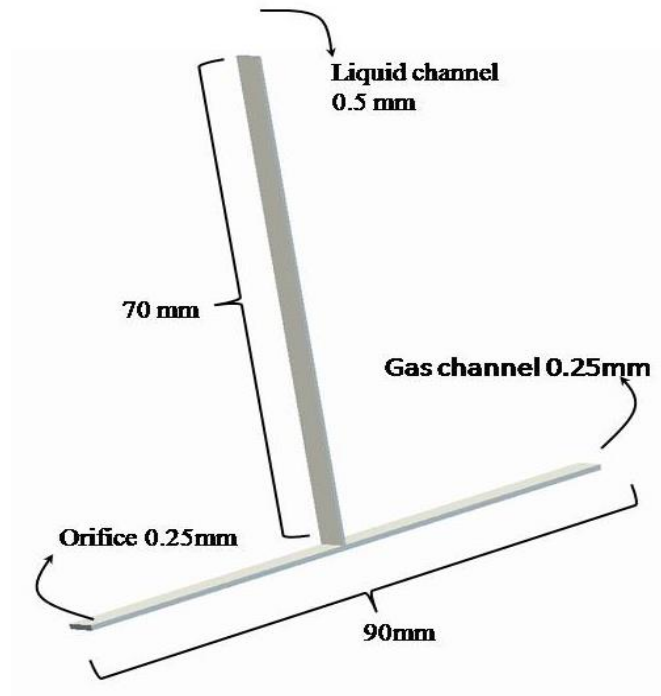


Figure 14: MF T-junction design

3.2.2 Fabrication of Microfluidic device

Final design was optimized after several trials using following materials for fabrication:

- Acrylic slabs
- Polyurethane
- Teflon tubes

3.2.2.1 Acrylic slabs

Pro E Design was fabricated on acrylic slabs. Channels of geometry were created on two slabs using specific laser parameters of speed, power and scan gap selected after optimization. at different parameters height of several depth was achieved and least height obtained was selected.

	Power	Speed	Depth obtained
1.	50W	100 mms-1	0.57mm
2.	40W	100 mms-1	0.38mm
3.	30W	100 mms-1	0.15mm

Table 1: Laser parameters and depth achieved

Scam gap was kept at 0.02 throughout. Two slabs having channels created through laser were then sealed together using sealants to obtain closed channels and checked for leakage by injecting water inside the channels using syringe.



Figure15: channels fabricated on acrylic slab

3.2.2.2 Polyurethane casting

Silicon cast was prepared by mixing 2 parts in (volumetric) ratio 1:1. Using pattern created on acrylic slab as master mold silicon mold was casted. Polyurethane (PU) 744D was prepared by mixing in ratio of 2:1 (volumetric) and poured into the silicon mold. Two pieces of PU were casted individually and then sealed together to obtain closed channel. This device made of PU was then checked for leakage again using syringe for injection of water.

Complete methodology is shown in Figure

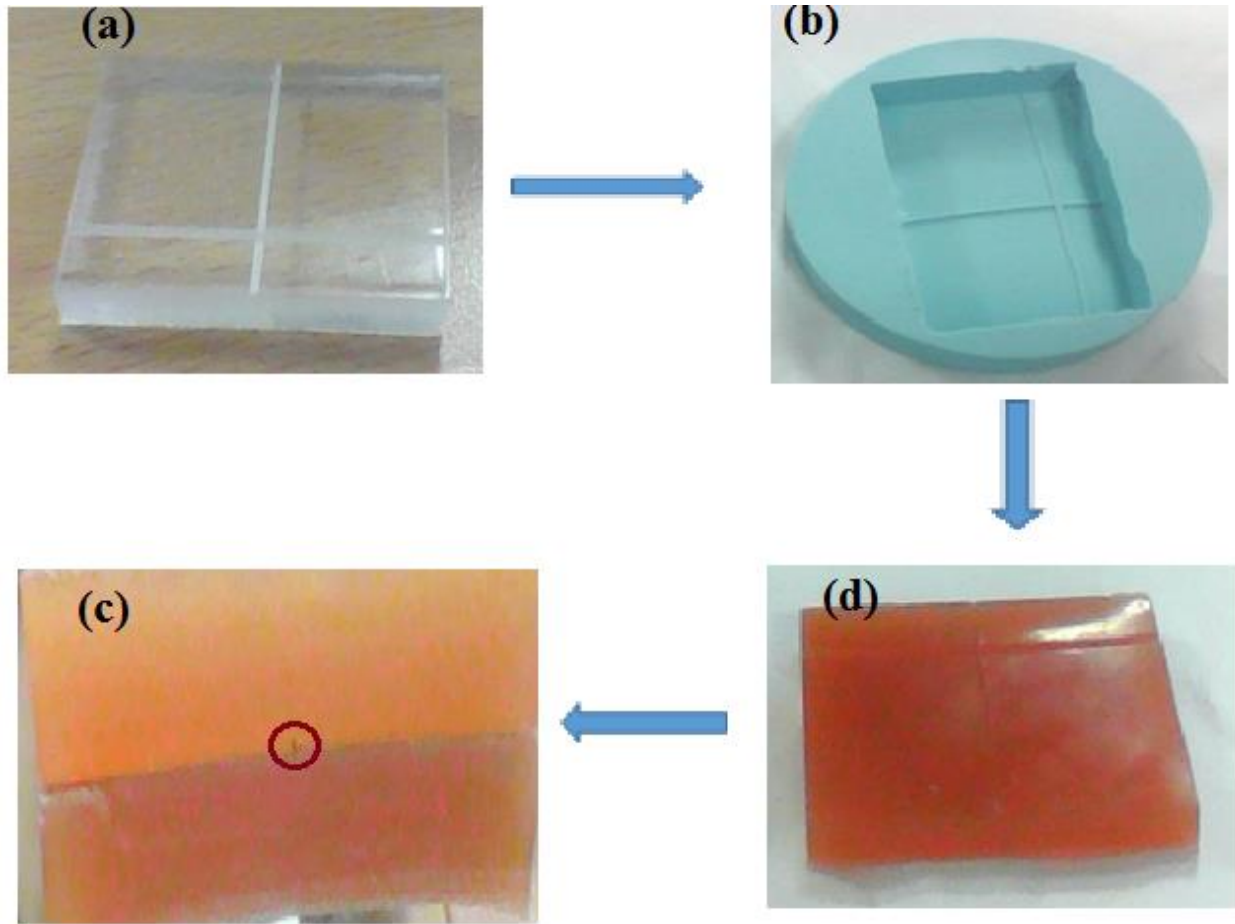


Figure 16 (a) Mater mold of acrylic (b) silicon mold (c) PU 744D casting (d) Two Pu744d pieces sealed together making pattern of channels

3.2.2.3 Teflon tubes

Two Teflon tubes of 50cm long were taken. One tube was inserted perpendicular to other one manually by cutting and soldering techniques. Three parts were then connected at a junction making a perfect T junction as shown in figure. External diameter of Teflon tube was 1mm and internal diameter was 0.5 mm to 0.8 mm .At the end another metallic tube of 350 micron was inserted at outlet of T-junction device. Junction was sealed using plastic tubing and further protected by setting T junction in a petri plate along with inlets and outlet connections. Polyurethane 744D after mixing two parts properly and poured into the petri plate and kept overnight. Device was ready to use. It was then tested for leakage.

After fabrication of microfluidic device an automated microfluidic setup was ready for generation of microbubbles.

3.3 Microbubble generation

Microbubbles were generated using Chitosan for shell and air at for core.

Two percentages of chitosan were used. Chitosan solutions were prepared in 1% glacial acetic acid .PH was maintained at 4.5 to 5. To make 1% chitosan solution 1g of chitosan was dissolved in 100ml of 1% acetic acid at 35-40°C with continuous stirring at 1000rpm for almost 2 hours until it dissolved completely. 2% chitosan solution was prepared in 1 % glacial acetic acid at 35 - 40°C with continuous stirring at 1100 rpm for 3 to 4 hours till it dissolved completely. Solutions were then filtered using Whatman® filter paper grade1 of thickness 180µm and pore size of 12µm.

For collection of bubbles glutaraldehyde was selected as it is best crosslinked for chitosan. Glutaraldehyde. It crosslinks the chitosan molecule as shown is figure:

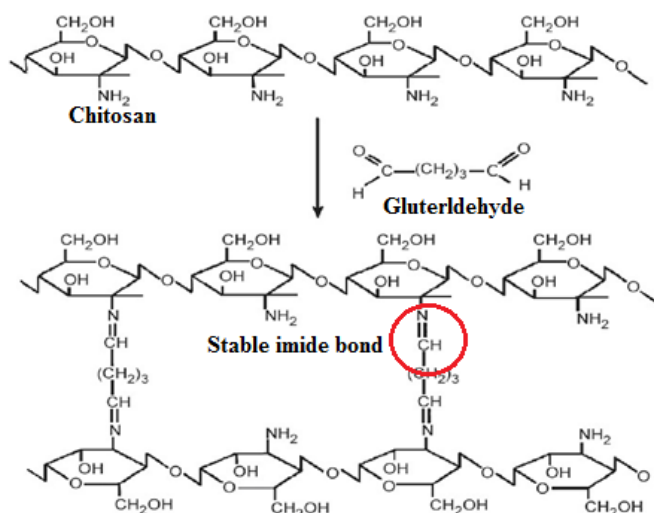


Figure 17: Crosslinking of chitosan with glutaraldehyde

Solutions of 0.5%, 1.5% and 2.5% glutaraldehyde in distilled water were prepared.

After preparation of solutions, one 3ml syringe was filled first with 1% Chitosan solution and other was filled with air. Both syringes were placed and fitted at their position on two separate syringe

pumps fabricated for introduction of fluids separately. Microfluidic device fabricated in step 2 was then connected to both syringes through Teflon tubing. Channel in line with outlet was connected to syringe filled with air and that perpendicular to main channel was connected to syringe filled with one percent chitosan. Flow rate was kept at 60 $\mu\text{l}/\text{min}$ through keypad attached to syringe pumps number of steps and time by giving input as number of steps and time in seconds. Flow rate of both gas and liquid phase was kept same. Bubbles started to generate that were collected first in 0.5 % glutaraldehyde, 1.5 % glutaraldehyde and then 2.5 % glutaraldehyde.

Bubbles were collected in above mentioned percentages of glutaraldehyde solution one by one in a beaker placed on hot plate (----) at 40°C and at continuous stirring to prevent aggregation of bubbles.

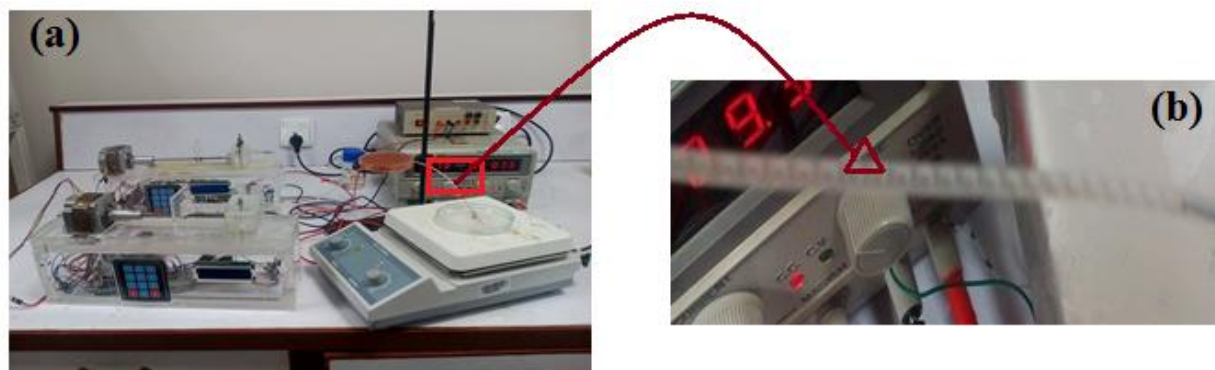


Figure: 18 (a) Microbubble generation through automated microfluidic setup (b) closed view bubbles flowing in out let

After 1% same procedure was followed for 2% chitosan solution. Device was washed with distilled water and acetone to remove any contamination inside the channels that may cause blockage and affect the bubble formation badly if not washed and dried properly before every step. All steps were done in triplicate.

3.4 Characterization

Microbubbles were generated successfully using gas as core and 1% and 2% chitosan as shell material. After collection bubbles were kept at continues stirring at 40°C for 30 mins and then washed using distilled water to get rid of any extra glutaraldehyde.

Optical microscopy was used for characterization. Images were taken using a high speed camera (MD35) attached to the microscope. Size of bubbles was measured using appropriate measuring scale. Calibration was done in micrometer desired measuring scale was micrometer. Polydispersity index was then calculated using formula.

Stability of bubbles were also noted by noting the time for how much they remain stable after washing.

4. RESULTS AND DISCUSSION

4.1 Design and Fabrication of syringe pump

Syringe pump was successfully designed and fabricated on acrylic sheet. Final assembled syringe pump is shown in figure

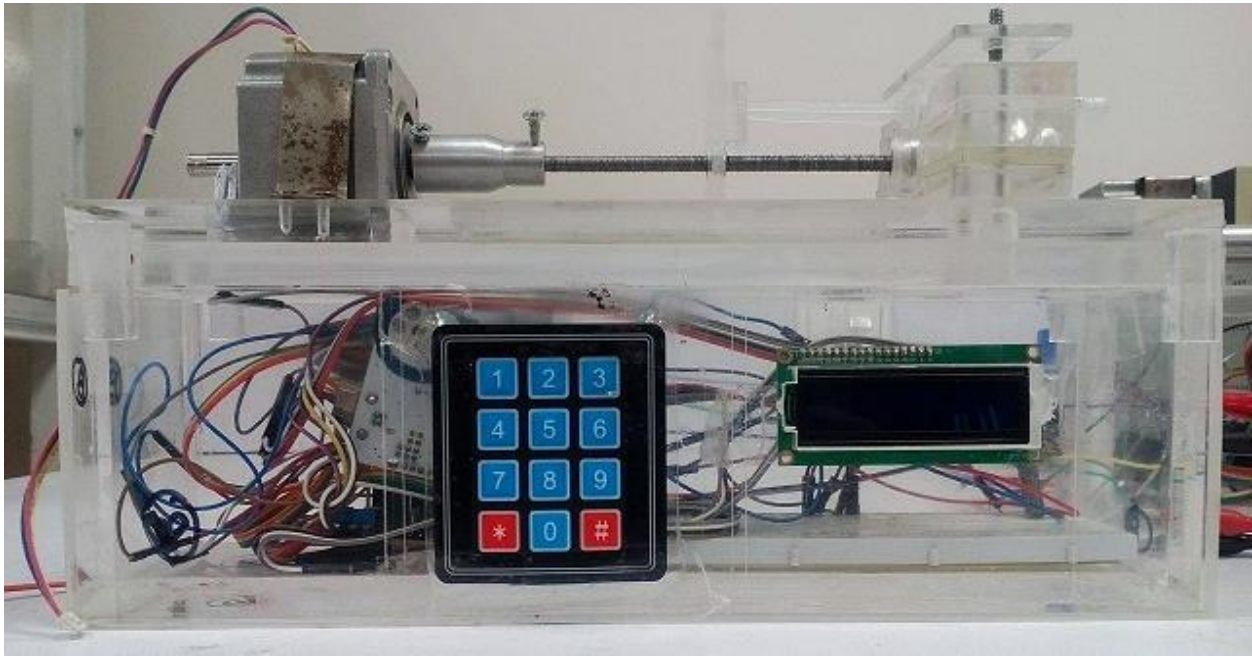


Figure 19: Final assembled syringe pump

The syringe pump was actuated by a stepper motor. Rotary to linear conversion was done via lead screw mechanism to attain a fine and smooth system operation.

We prefer using Stepper motor over simple DC motor because stepper motor allows to control steps (usually few degrees) while Simple DC motor control speed. Our requirement was very precise control over motor rotation. So number of steps were given with a time delay in milli seconds that was set according to required speed. Electric circuit was designed using micro controller and motor drive circuits. Initially we thought of designing a single chip solution to the required circuit i.e. Power, Controller, keypad, LED, VR and output motor Signal on one PCB and

Motor driver circuit on another PCB. ATmega328 was used for this as it can be easily programmed using ARDUINO UNO. We designed and simulated these circuits using PROTEUS ISIS. Once we arrived at an optimal design, Using PROTEUS ARES we printed PCBs for those circuits. They worked well for initial few tries but then they to show some error were with the PCB printed. Then we tried using ARDUINO UNO itself for this purpose and that worked well throughout. Stepper motor Driver Module was used to control stepper motor.

Stepper Motor selected was of 12v/1.93a rating after trying several motors having rating of 5v/0.5a, 12v/0.8a but these were not able to provide sufficient power to push the plunger. Now we placed our first motor (5V/0.5A) and tested circuit. The Motor wasn't able to provide enough power to push the injector. We changed the motors with those of high current ratings (12V/0.8A) but they also didn't worked well. Thus, we thought of using 12V/1.93A rating stepper motors and they finally worked well.

4.1.1 Calibration

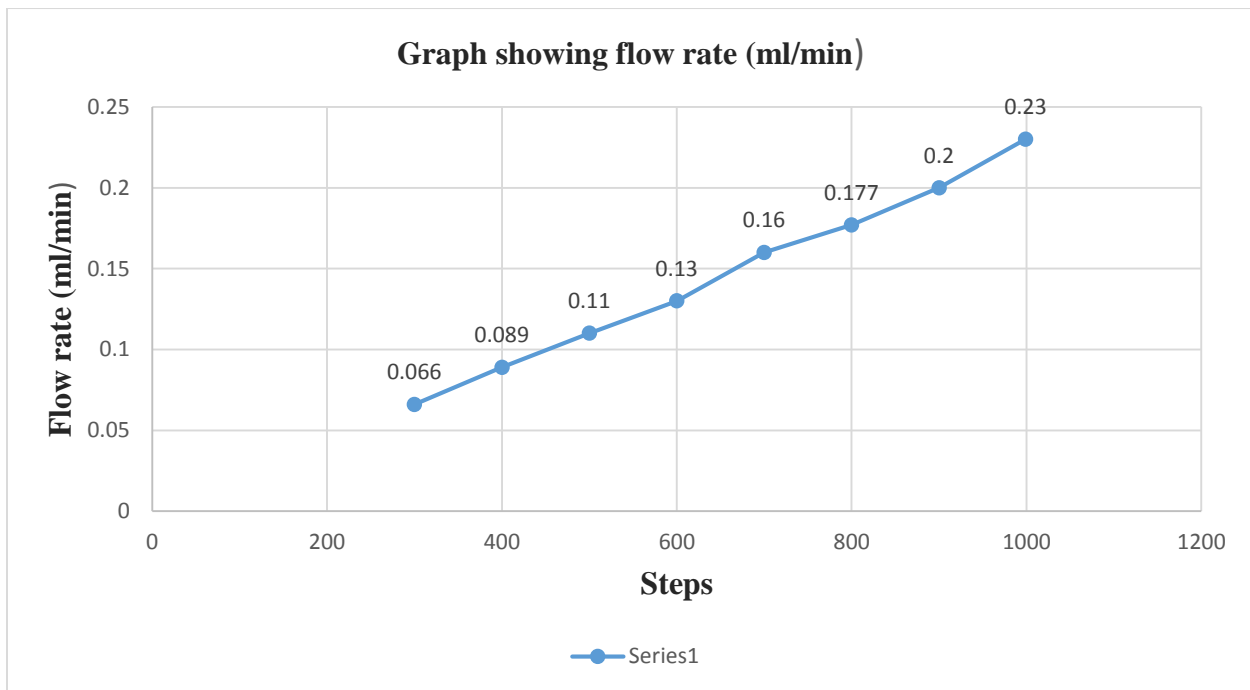


Figure 20: Graph showing Flow rate at various number of steps given per minute.

Commercially available pumps are very expensive but Pump fabricated here was very cost effective and measurement obtained was precise. Desired flow rate can be achieved. At 300 steps

Flow rate achieved was 0.066/min, at one step flow rate would be 0.00022 ml/min or $0.22 \mu\text{l/min}$ depending on cross section of syringe being used.

Another advantage of this syringe pump is that it can be updated with more features like pressure sensors and regulators etc. and is reprogrammable.

4.2 Design and Fabrication of Microfluidic Device

Optimized design after different trials is shown in figure

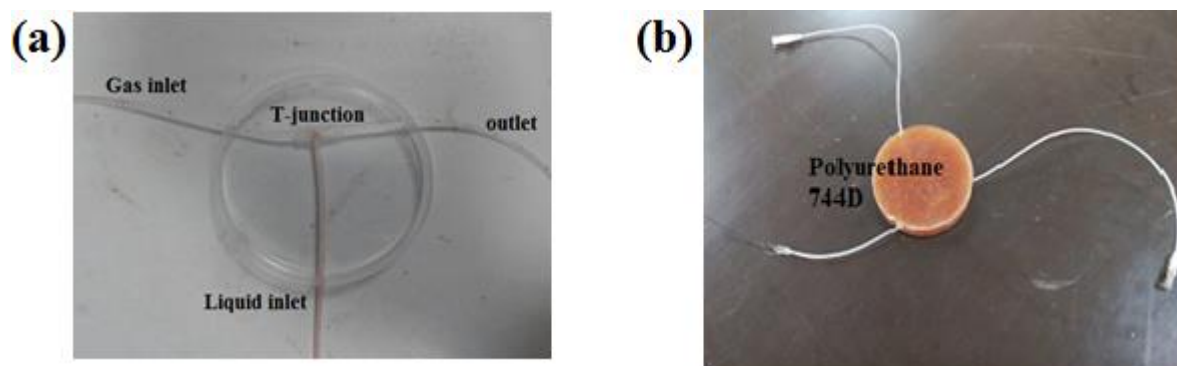


Figure 22: (a) MF T junction device (b) MF T junction protected by casting PU 744D

This was successful design. No any leakage was observed using this device while testing. Further it could be handled easily and could also bear pressure. The flowing inside Teflon tubing could also be seen easily with naked eye.

The main problem observed with acrylic and polyurethane 744D was leakage. Small Channels although could be fabricated on acrylic but upon sealing two slabs together misalignment occurred and leakage was seen. Further channels was not very smooth that caused the liquid to struck inside the channels at some places resulted in increase in pressure.

Same was the case with polyurethane 744D casting. Leakage and misalignment of channels was noted and polyurethane was coloured material so liquid flowing inside the channels could not be seen easily. We also tried capillary glass tubes that were inserted inside the fabricated on acrylic sheet but capillary tubes were very brittle and could not bear much pressure also its handling was difficult because of its brittle nature.

According to literature Polydimethylsiloxane (PDMS) has been the focus for fabricating MF devices using soft lithography technique [65]. It is used mainly because of it is optically transparent, and can also reversibly adhere to typical substrate used like silicon and glass. These properties made it predominant for 2D and 3D microchannel casting[66]. But the drawback of using PDMS is reduced chemical compatibility and less mechanical strength that limited its MF applications [66]. Additionally, soft lithography used for fabrication although is good for fabricating very small channels but it is expensive, method itself is also quite complex and not available everywhere. Glass microfluidic devices have fascinated consideration recently because of their bio compatibility, outstanding chemical robustness and optical properties but it also again requires complex and expensive photolithography process. This shortcoming was overcome now by researchers by using patterned cover slips and microscopic glass slides for fabrication of easy and low-cost MF chips [67].

Herein, we reported the design of very simple and cheap MF device with comfort of placement and aligning, based on Teflon tubes and polyurethane 744D, for generation of monodisperse MBs. The advantages of this approach is a simple fabrication and assemblage procedure and there is no need for expensive fabrication equipment. In future system can be further scaled down using Teflon tubes of less diameter that will be required for the generation of bubbles for in vivo studies.

The complete microfluidic setup fabricated in this study is shown in figure:

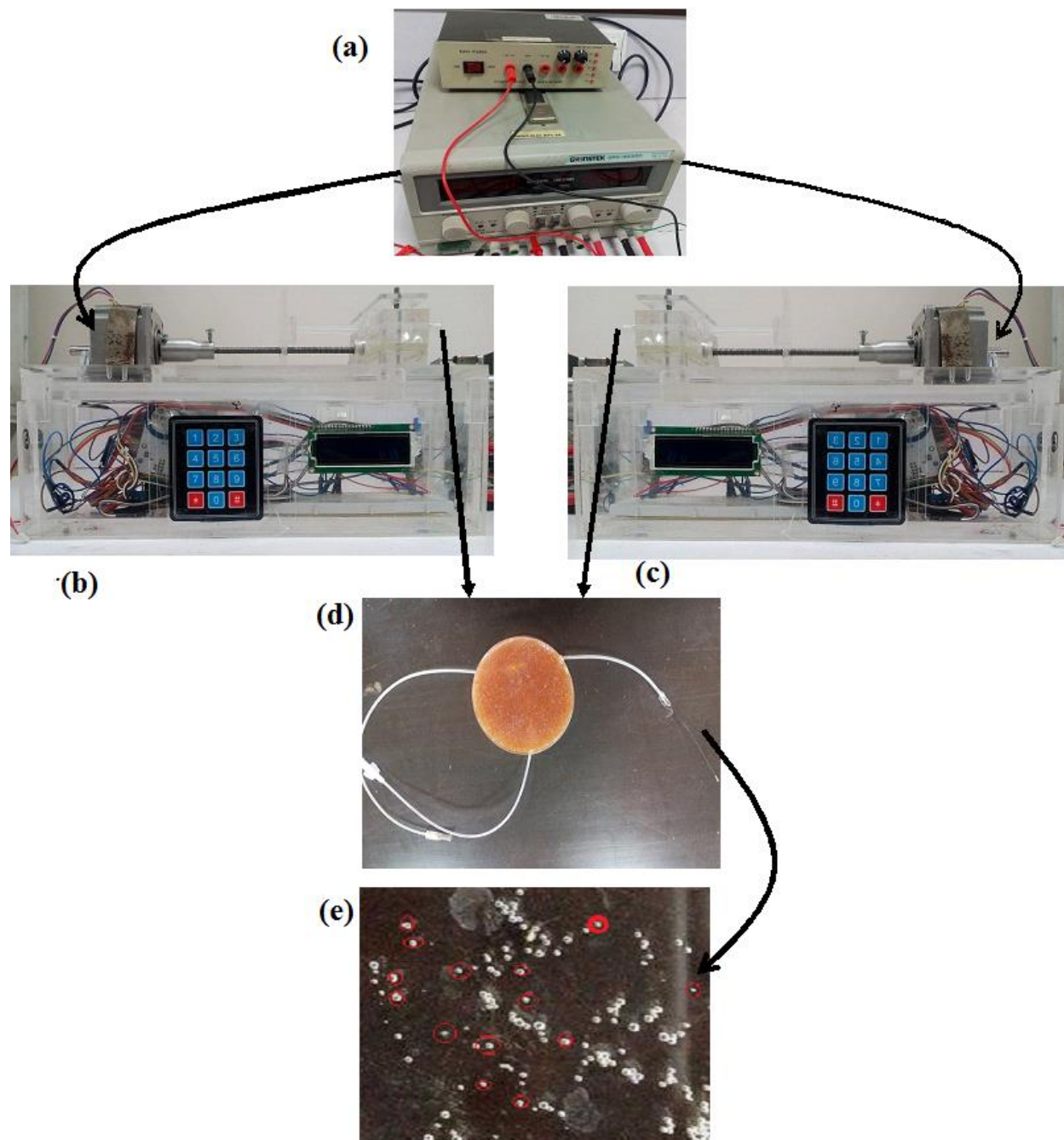


Figure 23: A complete MF setup (a) power supply (b) syringe pump for gas phase (c) syringe pump for liquid phase (d) MF device (e) Bubbles generated through this setup

4.3 Microbubble generation and Characterization

4.3.1 Optical microscopic images

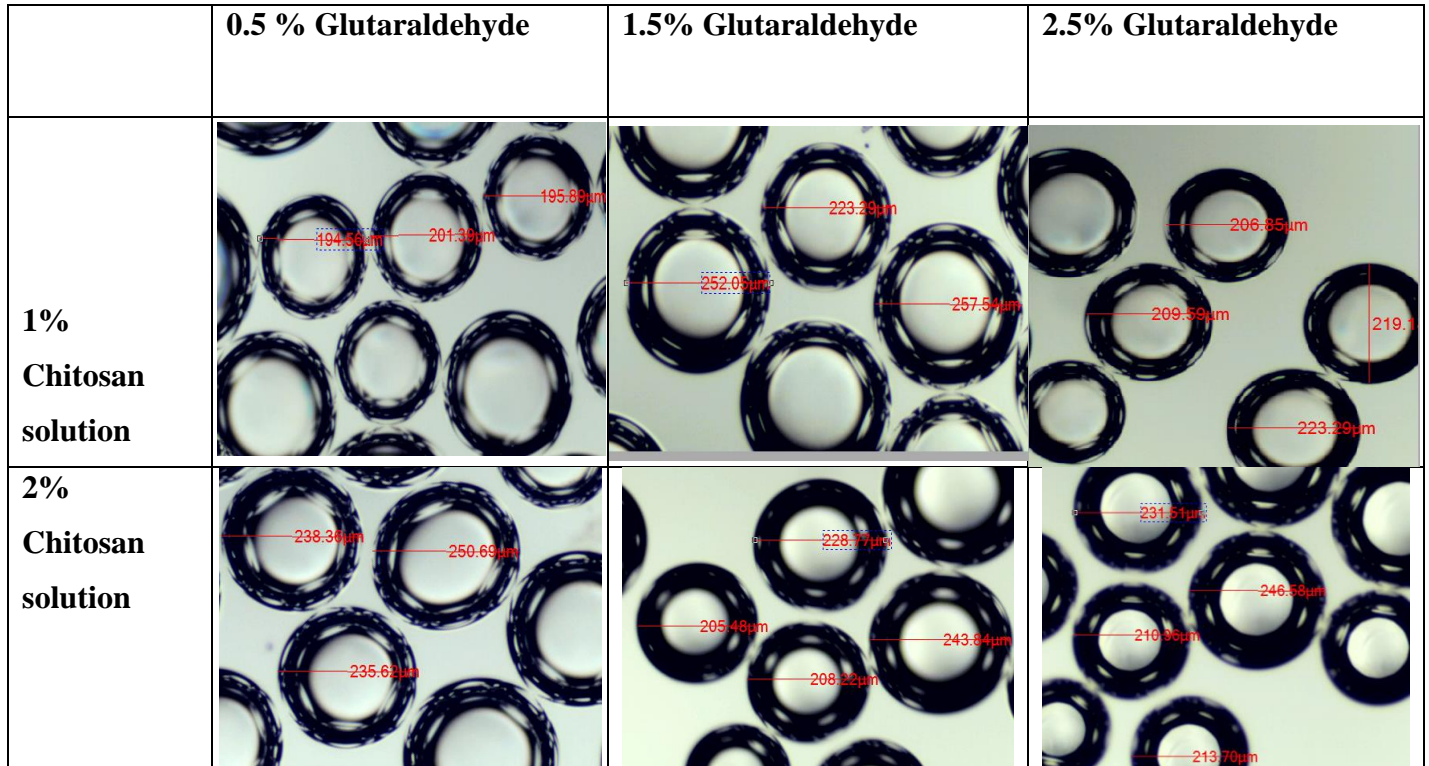


Figure 24: Microscopic images of 1%, 2% chitosan MBs in three different glutaraldehyde concentrations

Chitosan was selected for shell material because it is nontoxic and biocompatible so can be used intravenously in future if bubbles obtained would have size of $2\mu\text{m}$ to $5\mu\text{m}$.

Average size range of bubbles obtained was 200 μm to 260 μm

Chitosan %	Glutaraldehyde %		
	0.5%	1.5%	2.5%
1%	222 $\mu\text{m} \pm 16.38$	226.4 $\mu\text{m} \pm 15.76$	229.8 $\mu\text{m} \pm 15.03$
2%	228.9 $\mu\text{m} \pm 16.05$	230.5 $\mu\text{m} \pm 15.778$	231 $\mu\text{m} \pm 14.87$

Table 2: Average size of Chitosan Bubbles

4.3.2 Polydispersity index

Polydispersity index (sigma) values of bubble was calculated from the mean diameters of 20 bubbles and standard deviation.

Formula for polydispersity index is

Using following formula [16]

$$\sigma = \delta / d_{\text{avg}} \times 100\%$$

Where,

σ = Polydispersity index

δ = Standard deviation

D_{avg} = Average diameter of bubbles

Polydispersity index (sigma) values was found to be 6 % that was quite good than polydispersity obtained through sonication, agitation and other conventional methods. In contrast, the polydispersity indices for sonication and CHEDA were 50% and 30%. So monodispersity can only be achieved through microfluidic device under a controlled liquid and gas flow rates within a limited range. Out of these limits polydispersity may exceed [20],[17]. So high precision pumps are required for accurate flow control.

There was no notable difference shown at different concentrations of glutaraldehyde and also among two concentration of chitosan. A slight thickness of coating with 2% was though observed. The difference seen only in the stability time at 0.5%, 1.5% and 2% glutaraldehyde which is shown in table

Chitosan %	0.5 % Glut	1.5 % Glut	2.5 % Glut
1 % Chitosan	25 mins	1 hour 20 mins	2 hours
2% Chitosan	30 mins	1 hour 30 mins	2 hours 20 mins

Table3: stability of chitosan microbubbles

How shell of microbubbles shrink with time (after washing), can be seen from some images taken under optical microscope after every 30 minutes.

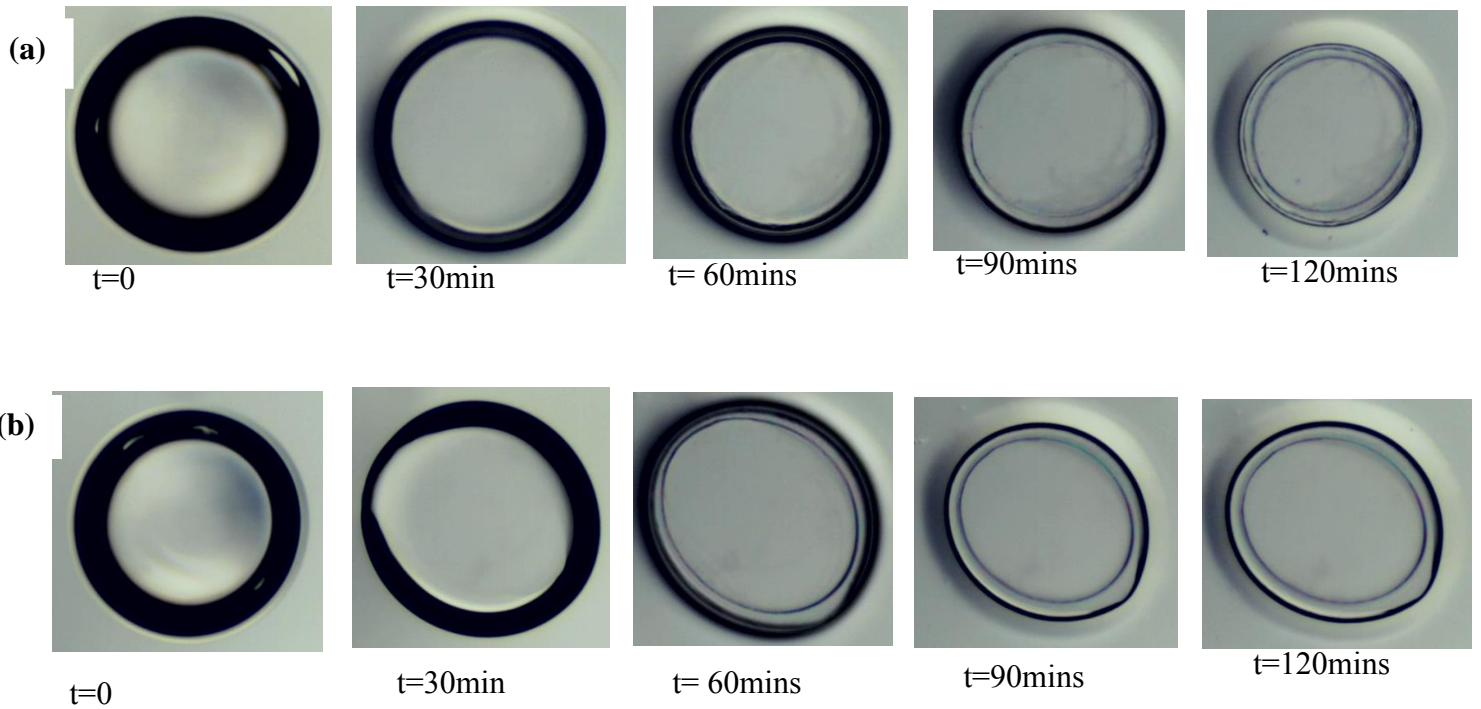


Figure 24: (a) 1 % chitosan Bubbles shrinking with time (b) 2% chitosan bubbles shrinking with time

MBs decrease in size in aqueous environment. Surface tension increase the pressure within the bubble and is inversely proportional to the diameter of bubble. Young-Laplace explained the relationship between pressure and diameter which is expressed by equation,[68]

$$P = P_l + 2\sigma/r$$

where

P = gas pressure

P_l = liquid pressure

σ = surface tension, and

r = radius of the bubble[68]

More Research work is still needed to understand the properties of microbubbles.

5. CONCLUSION

Automated microfluidic setup was developed. Setup consist of syringe pumps and MF device. Two syringe pumps were fabricated for feeding microfluidic device with gas and liquid phase through two inlets. MF device was fabricated using Teflon tubes had and outlet of 350 microns. By maintaining the constant flow rates throughout the process chitosan microbubbles with narrow size range of 200 μ m to 260 μ m were generated. Stability of chitosan bubbles was varying with increasing concentration of crosslinking agent that is glutaraldehyde. Bubbles generated using 2% chitosan and collected in 2.5 glutaraldehyde were found to be more stable than all other concentrations. Using this setup further studies can be carried out. That include modification in this setup to further scale down the size of bubbles either by fabricating device with very small dm channels and by changing the flow rates of both phases microbubbles so that bubbles with size range between 2 μ m to 5 μ m can be achieved which is requirement to be used for biomedical applications. Gas flow rate should be less then liquid to achieve further smaller bubbles. This can be made possible by regulating inline pressures of both phases.

REFERENCES

- [1] J. D. Ramsey, S. C. Jacobson, C. T. Culbertson, and J. M. Ramsey, "Protein Digests on Microfluidic Devices," vol. 75, no. 7, pp. 3758–3764, 2008.
- [2] J. Tan, S. W. Li, K. Wang, and G. S. Luo, "Gas-liquid flow in T-junction microfluidic devices with a new perpendicular rupturing flow route," *Chemical Engineering Journal*, vol. 146, no. 3, pp. 428–433, 2009.
- [3] W. D. Araujo, F. K. Schneider, and R. E. M. Morales, "Evaluation of stability and size distribution of sunflower oil-coated micro bubbles for localized drug delivery," *BioMedical Engineering OnLine*, vol. 11, no. 1, p. 71, 2012.
- [4] a. Manz, N. Graber, and H. M. Widmer, "Miniaturized total chemical analysis systems: A novel concept for chemical sensing," *Sensors and Actuators B: Chemical*, vol. 1, no. 1–6, pp. 244–248, 1990.
- [5] A. Mohammadkhah, L. M. Marquardt, S. E. Sakiyama-Elbert, D. E. Day, and A. B. Harkins, "Fabrication and characterization of poly-(ϵ)-caprolactone and bioactive glass composites for tissue engineering applications," *Materials Science and Engineering: C*, vol. 49, pp. 632–639, 2015.
- [6] Z. Fan, H. Ludi, and H. M. Widmers, "@ W'," vol. 7, no. 20, pp. 249–255, 1992.
- [7] S. Ramachandran, S. M. Shaheedha, G. Thirumurugan, and M. D. Dhanaraju, "Floating controlled drug delivery system of famotidine loaded hollow microspheres (microballoons) in the stomach.," *Current drug delivery*, vol. 7, no. 1, pp. 93–97, 2010.
- [8] M. J. Borrelli, W. D. O'Brien, E. Hamilton, M. L. Oelze, J. Wu, L. J. Bernock, S. Tung, H. Rokadia, and W. C. Culp, "Influences of microbubble diameter and ultrasonic parameters on in vitro sonothrombolysis efficacy," *Journal of Vascular and Interventional Radiology*, vol. 23, no. 12, pp. 1677–1684, 2012.

- [9] Y. Z. Zhao, H. D. Liang, X. G. Mei, and M. Halliwell, "Preparation, characterization and in vivo observation of phospholipid-based gas-filled microbubbles containing hirudin," *Ultrasound in Medicine and Biology*, vol. 31, no. 9, pp. 1237–1243, 2005.
- [10] B. Jiang, C. Gao, and J. Shen, "Polylactide hollow spheres fabricated by interfacial polymerization in an oil-in-water emulsion system," *Colloid and Polymer Science*, vol. 284, no. 5, pp. 513–519, 2006.
- [11] U. Farook, H. B. Zhang, M. J. Edirisinghe, E. Stride, and N. Saffari, "Preparation of microbubble suspensions by co-axial electrohydrodynamic atomization," *Medical Engineering and Physics*, vol. 29, no. 7, pp. 749–754, 2007.
- [12] R. Dangla, S. C. Kayi, and C. N. Baroud, "Droplet microfluidics driven by gradients of confinement.," *Proceedings of the National Academy of Sciences of the United States of America*, vol. 110, no. 3, pp. 853–8, 2013.
- [13] B. Dollet, W. Van Hoeve, J. P. Raven, P. Marmottant, and M. Versluis, "Role of the channel geometry on the bubble pinch-off in flow-focusing devices," *Physical Review Letters*, vol. 100, no. 3, 2008.
- [14] J. Prajapati and Y. Agrawal, "Synthesis, Characterization and Application of Microbubbles: a Review," *International Journal*, vol. 3, no. 06, pp. 1532–1543, 2012.
- [15] M. Borden, "NIH Public Access," *Bubble Sci Eng Technol.*, vol. 1, pp. 3–17, 2010.
- [16] K. Hettiarachchi, E. Talu, M. L. Longo, P. a Dayton, and A. P. Lee, "On-chip generation of microbubbles as a practical technology for manufacturing contrast agents for ultrasonic imaging.," *Lab on a chip*, vol. 7, no. 4, pp. 463–468, 2007.
- [17] E. Talu, K. Hettiarachchi, R. L. Powell, A. P. Lee, P. a. Dayton, and M. L. Longo, "Maintaining monodispersity in a microbubble population formed by flow-focusing," *Langmuir*, vol. 24, no. 5, pp. 1745–1749, 2008.

- [18] M. Lee, E. Y. Lee, D. Lee, and B. J. Park, "Stabilization and fabrication of microbubbles: applications for medical purposes and functional materials," *Soft Matter*, vol. 11, no. 11, pp. 2067–2079, 2015.
- [19] K. S. Suslick, Y. Didenko, M. M. Fang, T. Hyeon, K. J. Kolbeck, W. B. McNamara, M. M. Mdleleni, and M. Wong, "Acoustic cavitation and its chemical consequences," *Philosophical Transactions of the Royal Society A: Mathematical, Physical and Engineering Sciences*, vol. 357, no. 1751, pp. 335–353, 1999.
- [20] M. W. Grinstaff and K. S. Suslick, "Air-filled proteinaceous microbubbles: synthesis of an echo-contrast agent.," *Proceedings of the National Academy of Sciences of the United States of America*, vol. 88, no. September, pp. 7708–7710, 1991.
- [21] W. L. Nyborg, "Biological effects of ultrasound: Development of safety guidelines. Part II: General review," *Ultrasound in Medicine and Biology*, vol. 27, no. 3, pp. 301–333, 2001.
- [22] M. R. Böhmer, R. Schroeders, J. a M. Steenbakkers, S. H. P. M. de Winter, P. a. Duineveld, J. Lub, W. P. M. Nijssen, J. a. Pikkemaat, and H. R. Stapert, "Preparation of monodisperse polymer particles and capsules by ink-jet printing," *Colloids and Surfaces A: Physicochemical and Engineering Aspects*, vol. 289, pp. 96–104, 2006.
- [23] E. Stride and M. Edirisinghe, "Novel microbubble preparation technologies," 2008.
- [24] S. M. Joscelyne and G. Trägårdh, "Membrane emulsification - A literature review," *Journal of Membrane Science*, vol. 169, no. 1, pp. 107–117, 2000.
- [25] M. Kukizaki and M. Goto, "Spontaneous formation behavior of uniform-sized microbubbles from Shirasu porous glass (SPG) membranes in the absence of water-phase flow," *Colloids and Surfaces A: Physicochemical and Engineering Aspects*, vol. 296, pp. 174–181, 2007.
- [26] "S0376738806002432 (1)." .

- [27] T. Kawakatsu, G. Trägårdh, C. Trägårdh, M. Nakajima, N. Oda, and T. Yonemoto, “The effect of the hydrophobicity of microchannels and components in water and oil phases on droplet formation in microchannel water-in-oil emulsification,” *Colloids and Surfaces A: Physicochemical and Engineering Aspects*, vol. 179, pp. 29–37, 2001.
- [28] C. Chen, Y. Zhu, P. W. Leech, and R. Manasseh, “Production of monodispersed micron-sized bubbles at high rates in a microfluidic device,” *Applied Physics Letters*, vol. 95, no. 14, 2009.
- [29] K. Pancholi, E. Stride, and M. Edirisinghe, “Dynamics of Bubble Formation in Highly Viscous Liquids,” *Time*, vol. 1, no. 7, pp. 4388–4393, 2008.
- [30] E. Stride, K. Pancholi, M. J. Edirisinghe, and S. Samarasinghe, “Increasing the nonlinear character of microbubble oscillations at low acoustic pressures,” *Journal of the Royal Society, Interface / the Royal Society*, vol. 5, no. 24, pp. 807–811, 2008.
- [31] J. Rodríguez-Rodríguez, A. Sevilla, C. Martínez-Bazán, and J. M. Gordillo, “Generation of Microbubbles with Applications to Industry and Medicine,” *Annual Review of Fluid Mechanics*, vol. 47, no. 1, pp. 405–429, 2015.
- [32] J. H. Xu, S. W. Li, C. Tostado, W. J. Lan, and G. S. Luo, “Preparation of monodispersed chitosan microspheres and in situ encapsulation of BSA in a co-axial microfluidic device,” *Biomedical Microdevices*, vol. 11, no. 1, pp. 243–249, 2009.
- [33] Y. Cui and P. a. Campbell, “Towards monodisperse microbubble populations via microfluidic chip flow-focusing,” *Proceedings - IEEE Ultrasonics Symposium*, pp. 1663–1666, 2008.
- [34] S. L. Anna, N. Bontoux, and H. a. Stone, “Formation of dispersions using ‘flow focusing’ in microchannels,” *Applied Physics Letters*, vol. 82, no. 3, pp. 364–366, 2003.

- [35] A. M. Gañán-Calvo, “Perfectly monodisperse microbubbling by capillary flow focusing: An alternate physical description and universal scaling,” *Physical Review E - Statistical, Nonlinear, and Soft Matter Physics*, vol. 69, no. 2 2, pp. 1–3, 2004.
- [36] J. Wan, A. Bick, M. Sullivan, and H. a. Stone, “Controllable microfluidic production of microbubbles in water-in-oil emulsions and the formation of porous microparticles,” *Advanced Materials*, vol. 20, no. 17, pp. 3314–3318, 2008.
- [37] T. Fu, D. Funfschilling, Y. Ma, and H. Z. Li, “Scaling the formation of slug bubbles in microfluidic flow-focusing devices,” *Microfluidics and Nanofluidics*, vol. 8, no. 4, pp. 467–475, 2010.
- [38] E. Castro-Hernández, W. van Hoeve, D. Lohse, and J. M. Gordillo, “Microbubble generation in a co-flow device operated in a new regime.,” *Lab on a chip*, vol. 11, no. 12, pp. 2023–2029, 2011.
- [39] J. L. Chen, A. H. Dhanaliwala, S. Wang, and J. A. Hossack, “Parallel Output , Liquid Flooded Flow-Focusing Microfluidic Device for Generating Monodisperse Microbubbles within a Catheter,” pp. 160–163, 2011.
- [40] S. Wang, H. Ali, L. Johnny, and J. A. Hos, “ptimal Micro bubble e Production n Rate from a Flow-F Focusi ng Mi croflu uidic D Device as a F Functio on of Nozz zle Siz ze , Gas s Press sure , a and Liq uid F low R Rate,” pp. 164–167, 2011.
- [41] a M. Gañán-Calvo and J. M. Gordillo, “Perfectly monodisperse microbubbling by capillary flow focusing.,” *Physical review letters*, vol. 87, no. 27 Pt 1, p. 274501, 2001.
- [42] S. Wang, A. H. Dhanaliwala, and J. a. Hossack, “Modeling microbubble production rates from expanding nozzle flow-focusing microfluidic devices,” *IEEE International Ultrasonics Symposium, IUS*, vol. 2, no. 1, pp. 667–670, 2012.
- [43] A. Salari, M. Azad, F. Shalchi, and M. B. Shafii, “An Experimental Study of the Effect of Channels Angle on Bubble Formation in Microchannel Flow Focusing Geometry,” pp. 276–277, 2012.

- [44] A. J. Dixon, A. H. Dhanaliwala, J. L. Chen, and J. a. Hossack, “Enhanced Intracellular Delivery of a Model Drug Using Microbubbles Produced by a Microfluidic Device,” *Ultrasound in Medicine and Biology*, vol. 39, no. 7, pp. 1267–1276, 2013.
- [45] L. Wang, Y. Zhang, and L. Cheng, “Magic microfluidic T-junctions: Valving and bubbling,” *Chaos, Solitons and Fractals*, vol. 39, no. 4, pp. 1530–1537, 2009.
- [46] S. Wang, A. H. Dhanaliwala, J. L. Chen, and J. a. Hossack, “Production rate and diameter analysis of spherical monodisperse microbubbles from two-dimensional, expanding-nozzle flow-focusing microfluidic devices,” *Biomicrofluidics*, vol. 7, no. 1, 2013.
- [47] M. Parhizkar, M. Edirisinghe, and E. Stride, “Effect of operating conditions and liquid physical properties on the size of monodisperse microbubbles produced in a capillary embedded T-junction device,” *Microfluidics and Nanofluidics*, vol. 14, no. 5, pp. 797–808, 2013.
- [48] H. Song and R. F. Ismagilov, “Millisecond Kinetics on a Microfluidic Chip Using Nanoliters of Reagents,” *Journal of the American Chemical Society*, vol. 125, no. 47, pp. 14613–14619, 2003.
- [49] C. J. Gerdt, D. E. Sharoyan, and R. F. Ismagilov, “A synthetic reaction network: Chemical amplification using nonequilibrium autocatalytic reactions coupled in time,” *Journal of the American Chemical Society*, vol. 126, no. 20, pp. 6327–6331, 2004.
- [50] B. Zheng, L. S. Roach, and R. F. Ismagilov, “Screening of protein crystallization conditions on a microfluidic chip using nanoliter-size droplets,” *Journal of the American Chemical Society*, vol. 125, no. 37, pp. 11170–11171, 2003.
- [51] D. Dendukuri, K. Tsoi, T. A. Hatton, and P. S. Doyle, “Controlled synthesis of nonspherical microparticles using microfluidics,” *Langmuir*, vol. 21, no. 6, pp. 2113–2116, 2005.
- [52] S. Okushima, T. Nisisako, T. Torii, and T. Higuchi, “Controlled production of monodisperse double emulsions by two-step droplet breakup in microfluidic devices,” *Langmuir*, vol. 20, no. 23, pp. 9905–9908, 2004.

- [53] T. Nisisako, T. Torii, and T. Higuchi, "Droplet formation in a microchannel network.," *Lab on a chip*, vol. 2, no. 1, pp. 24–26, 2002.
- [54] P. Garstecki, a M. Gañán-Calvo, and G. M. Whitesides, "Formation of bubbles and droplets in microfluidic systems," *Bulletin of the Polish Academy of Sciences*, vol. 53, no. 4, pp. 361–372, 2005.
- [55] J. H. Xu, S. W. Li, Y. J. Wang, and G. S. Luo, "Controllable gas-liquid phase flow patterns and monodisperse microbubbles in a microfluidic T-junction device," *Applied Physics Letters*, vol. 88, no. 13, pp. 17–20, 2006.
- [56] E. Stride and M. Edirisinghe, "Novel preparation techniques for controlling microbubble uniformity: A comparison," *Medical and Biological Engineering and Computing*, vol. 47, no. 8, pp. 883–892, 2009.
- [57] K. Wang, Y. C. Lu, J. Tan, B. D. Yang, and G. S. Luo, "Generating gas/liquid/liquid three-phase microdispersed systems in double T-junctions microfluidic device," *Microfluidics and Nanofluidics*, vol. 8, no. 6, pp. 813–821, 2010.
- [58] L. Yang, K. Wang, J. Tan, Y. Lu, and G. Luo, "Experimental study of microbubble coalescence in a T-junction microfluidic device," *Microfluidics and Nanofluidics*, vol. 12, no. 5, pp. 715–722, 2012.
- [59] M. Parhizkar, E. Stride, and M. Edirisinghe, "Preparation of monodisperse microbubbles using an integrated embedded capillary T-junction with electrohydrodynamic focusing.," *Lab on a chip*, pp. 2437–2446, 2014.
- [60] H. Peng, Z. Xu, S. Chen, Z. Zhang, B. Li, and L. Ge, "An easily assembled double T-shape microfluidic devices for the preparation of submillimeter-sized polyacronitrile (PAN) microbubbles and polystyrene (PS) double emulsions," *Colloids and Surfaces A: Physicochemical and Engineering Aspects*, vol. 468, pp. 271–279, 2015.

- [61] T. Nisisako, T. Torii, T. Takahashi, and Y. Takizawa, "Synthesis of monodisperse bicolored janus particles with electrical anisotropy using a microfluidic co-flow system," *Advanced Materials*, vol. 18, no. 9, pp. 1152–1156, 2006.
- [62] R. Xiong, M. Bai, and J. N. Chung, "Formation of bubbles in a simple co-flowing micro-channel," *Journal of Micromechanics and Microengineering*, vol. 17, no. 5, pp. 1002–1011, 2007.
- [63] K. Wang, L. Xie, Y. Lu, and G. Luo, "Generating microbubbles in a co-flowing microfluidic device," *Chemical Engineering Science*, vol. 100, pp. 486–495, 2013.
- [64] W.-T. Wang, R. Chen, J.-H. Xu, Y.-D. Wang, and G.-S. Luo, "One-step microfluidic approach for controllable production of gas-in-water-in-oil (G/W/O) double emulsions and hollow hydrogel microspheres," *RSC Advances*, vol. 4, no. 32, p. 16444, 2014.
- [65] K. Haraldsson, *Fabrication of polymeric microfluidic devices via photocurable liquid monomers*. 2005.
- [66] K. Regehr, M. Domenech, J. Koepsel, K. Craver, S. Ellison-Zelski, W. Murphy, L. Schuler, E. Alarid, and D. J. Beebe, "Biological implications of polydimethylsiloxane-based microfluidic cell culture," *Lab Chip*, vol. 9, no. 15, pp. 2132–2139, 2009.
- [67] X. Yi, R. Kodzius, X. Gong, K. Xiao, and W. Wen, "A simple method of fabricating mask-free microfluidic devices for biological analysis," *Biomicrofluidics*, vol. 4, pp. 1–8, 2010.
- [68] M. Takahashi, T. Kawamura, Y. Yamamoto, H. Ohnari, S. Himuro, and H. Shakutsui, "Effect of Shrinking Microbubble on Gas Hydrate Formation," *The Journal of Physical Chemistry B*, vol. 107, no. 10, pp. 2171–2173, 2003.